



# Use of Auxetic Infill Structures for the Compensation of Shrinkage in Fused Filament Fabrication Process

Rahman Uncu<sup>1,2</sup> , Mehmet Canberk Bacikoglu<sup>1,2</sup> , Burak Caliskan<sup>1,2</sup> ,  
and Ulas Yaman<sup>1</sup> 

<sup>1</sup> Department of Mechanical Engineering, Middle East Technical University, Ankara 06800, Turkey

uyaman@metu.edu.tr

<sup>2</sup> Radar and Electronic Warfare Systems, ASELSAN, Ankara 06830, Turkey

**Abstract.** The polymer parts fabricated by Fused Filament Fabrication (FFF) process deteriorated noticeably in terms of dimensional accuracy due to the thermal processes during the fabrication and cooling phases. Commonly, researchers tend to concentrate on modifying the CAD model or fabricating the parts larger than the nominal then post-processing the artifacts to compensate for shrinkage. This paper investigates the effects of auxetic infill structures on shrinkage compensation. Parts with different internal geometries and infill structures were designed and fabricated via FFF using polylactic acid material. Critical dimensions of these parts were measured on a Coordinate Measuring Machine to observe the effects of different infill patterns on the dimensional accuracy of the parts. Measurement results showed that using an auxetic infill pattern with a symmetrical layout improves the accuracy of the parts significantly.

**Keywords:** Fused Filament Fabrication · Auxetic structures · Shrinkage · Dimensional accuracy · Infill patterns

## 1 Introduction

Additive Manufacturing (AM) processes are going to be among the leading manufacturing technologies in near future considering the increased availability and interest on them. In this evolution, these technologies should be able to fabricate final products as well as prototypes. Lower and inconsistent dimensional accuracy is the main concern of AM technologies if the fabricated parts were to be used as the final products.

Although there are various sources of dimensional errors in Fused Filament Fabrication (FFF), such as the quality of the nozzle, positioning accuracy, staircase effect, etc., the main contribution is due to the shrinkage of extruded beads. In this AM process, the temperature of the filament material is increased to the values close to the melting point in the chamber and after the extrusion, the temperature is decreased due to convection and conduction. Temperature change in the fabricated parts causes thermal contraction, which is not linear due to the nonhomogeneous heat distribution. This imbalance results

in residual stresses within the part [1, 2]. In conclusion, the dimensional accuracy of the FFF printed parts alters significantly due to shrinkage.

The easiest and most conventional way to improve the dimensional accuracy in the FFF process is printing 3D parts larger than the nominal size and using post-processing methods to obtain the desired geometry. This approach is highly time-consuming and costly since a secondary operation is a must. Another option is using structured infill patterns to compensate for shrinkage. Yaman [3] used this approach and managed to improve the dimensional accuracy of parts. Schmutzler et al. [4] proposed a different approach to compensate shrinkage problem in FFF. In their method, dimensional accuracy can be enhanced with pre-deformation of the construction data. In this paper, we have proposed to use auxetic infill patterns to increase the accuracy of the parts fabricated with FFF. The related research is elaborated in terms of the dimensional accuracy of additively manufactured parts and the use of auxetic structures in AM applications.

### 1.1 Dimensional Accuracy of Additively Manufactured Parts

3D printed artifacts should have acceptable dimensional accuracy and tolerances to be used in assemblies. Generally, many AM processes have some problems regarding manufacturing the parts with required tolerances when compared to the conventional machining operations. For example, temperature gradients in the FFF process result in the shrinkage of the fabricated parts, which greatly affects the accuracy of these artifacts [5]. A well-known approach for this issue is to obtain a correlation between the designed and manufactured parts in terms of some parameters, modify the CAD model accordingly to compensate for the shrinkage and finally obtain the part with desired dimensions. In one of these studies, Noriega et al. [6] manufactured parts having nested squares inside with the FFF type of 3D printer and measured the distances between two parallel faces on a Coordinate Measuring Machine (CMM). They later utilized these results to train their Artificial Neural Networks. According to the feedback from their network, the dimensions of the CAD models are adjusted to fabricate end-use parts with higher dimensional accuracy. After these adjustments, obtained results revealed that the manufacturing errors on the external dimensions of the products were decreased by 47.4%, and regarding the internal dimensions a reduction of 31.9% was observed. In a similar approach, Huang et al. [7] focused on modifying the CAD models to compensate for the shrinkage of parts fabricated via the Stereolithography (SLA) type of AM. In their approach, they tried to model shrinkage and proposed a way to compensate for cylindrical objects. According to the results, for the compensated part, average and standard deviations of shrinkage were decreased to 10% of the uncompensated part.

As another approach to this problem, Yaman [3] studied minimizing inaccuracy of the inner features of the parts fabricated by the FFF process. He modified the interior structure of the parts to compensate for the shrinkage instead of adjusting the outer dimensions of the artifacts. This approach was tested with three different specimens having circular and rectangular inner features. According to the measurements on the CMM, up to 80% decrease in shrinkage of interior features was obtained. In a similar approach to Yaman [3], Dilberoglu et al. [1] also studied compensating shrinkage by implementing some auxiliary lines between inner features and outer boundaries of the parts. They compared this infill structure with a triangular infill pattern. Parts with two different inner features

were manufactured with these infills. According to the measurements, the accuracy of the parts fabricated with the proposed infill outperforms the parts with triangular infill in all the cases.

## 1.2 Use of Auxetic Structures in Additive Manufacturing

When fabricating objects with AM methods, cellular interior layouts are mostly preferred since unit cells having lightweight can undergo a large amount of stress and deformation while adequately dissipating the energy [8]. Honeycomb is a good example of these structures and can be found in an extensive range of applications from nature to composite structures, automotive-aerospace applications, and energy absorption mechanisms [9]. The studies on interior cells led to the development of auxetic structures which have a negative Poisson's ratio. Auxetic structures have enhanced mechanical properties such as toughness, stiffness, fatigue, and shear stiffness. AM technologies are fairly suitable to fabricate auxetic structures since the design limitations are far less compared to the conventional methods. Hassanin et al. [10] used Direct Metal Laser Melting with NiTi to manufacture 3D re-entrant structures. It is used to improve the ballistic performance considering the energy absorption property of the auxetic structures. The study signifies that the 3D printed part has better ballistic performance than the conventional steel armors. Maran et al. [11] used Direct Metal Laser Sintering to produce a variety of re-entrant honeycomb lattices. After the fabrication, they inspected the specimens' mechanical properties such as density, dimensional accuracy, elastic modulus, yield stress, Poisson's ratio, and porosity. The study demonstrates that the auxetic lattices can be successfully 3D printed via powder bed fusion processes.

FFF is the most frequently used 3D printing technology considering its availability and low cost. Various studies were conducted to analyze the performances of auxetic structures using the FFF method. Wagner et al. [12] produced heat-stimulated 4D auxetic structures using FFF. The interior cells were re-entrant honeycomb. The study demonstrated that it is possible to obtain area changes up to 200% in auxetic structures fabricated with FFF. Another research on FFF was conducted by Lvov et al. [13]. They fabricated auxetic and non-auxetic lattice structures and conducted compression tests on them. The research confirmed that the auxetic structures are more convenient for applications needing finer mechanical energy dissipation.

The remainder of the paper is organized as follows. The proposed approach is elaborated in Sect. 2 with the measurements on the CMM. Then, in Sect. 3 the paper is concluded with comments on the obtained results and future predictions.

## 2 Proposed Approach and Results

It is proposed to use auxetic infill structures to increase the dimensional accuracy of parts fabricated via FFF. This was tested for two different hole types (circular and square) and four different infill structures namely star honeycomb (auxetic), re-entrant honeycomb (auxetic), gyroid, and triangular (cross-hatched). A total of eight test parts were designed in Rhinoceros3D and Grasshopper3D in a parametric manner. The parts were 3D printed using Ultimaker 3 Extended FFF 3D printer with PLA material, and they are shown in

Fig. 1. Their infill unit cells are given in Fig. 2, which are star honeycomb (parts 1 and 5), re-entrant honeycomb (parts 2 and 6), gyroid (parts 3 and 7), and triangular (parts 4 and 8). These parts are all square in shape with a size of 100 mm and a thickness of 10 mm. Circular holes have diameters of 40 mm, and the size of the square holes is 30 mm. CMM measurements, as seen in Fig. 3, were taken to evaluate the dimensional accuracy of the fabricated parts. The type of the CMM used is Hexagon Delta Slant. Measurements were not taken at a single level (Tables 1 and 2), but three levels (Tables 3 and 4) were considered to examine the effects of the heated build platform on the shrinkage.

According to the measurements, the outer dimensions of the parts in the  $x$  and  $y$  axes are similar to each other for all the test cases except the parts with a re-entrant honeycomb infill pattern. This is due to the asymmetric nature of this infill structure in the  $x$  and  $y$  axes. Regarding the outer dimensions, the best accuracy was obtained with the parts having a star honeycomb infill pattern. The parts with triangular, re-entrant honeycomb and gyroid infill patterns are the second, third and fourth, respectively, when ordered according to their accuracy as can be inferred from Tables 1 and 2. Furthermore, the accuracy of the 3D printed parts at the outer dimensions is getting better with an increase in height which can be seen in Fig. 3 as  $z$ -axis (Fig. 3).

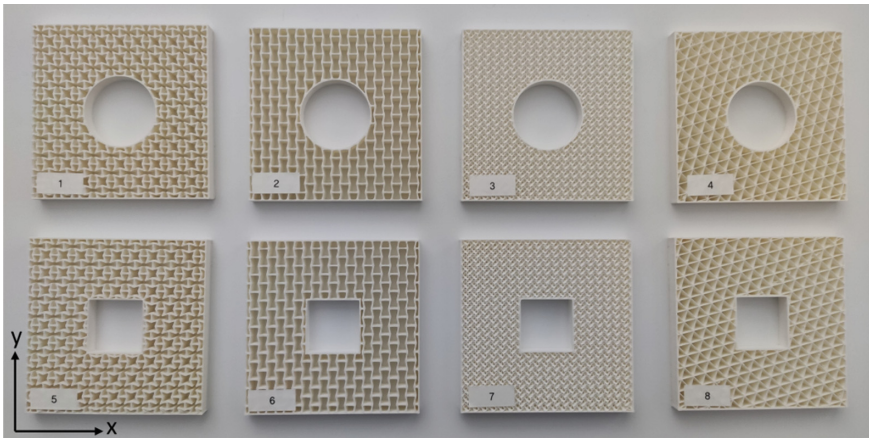


Fig. 1. 3D printed test parts.

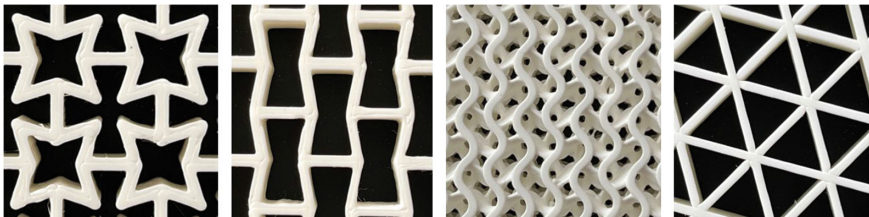
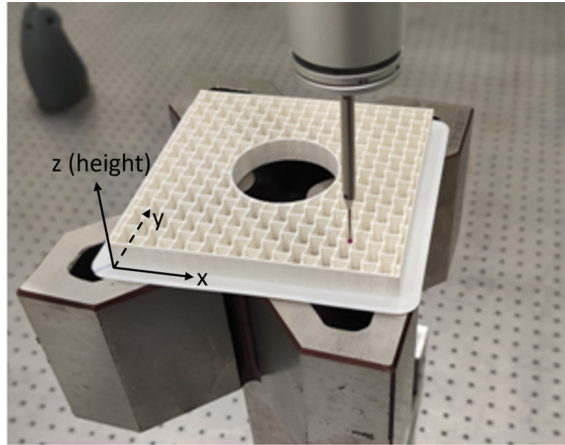


Fig. 2. Unit cell structures.



**Fig. 3.** Measurement of a sample test part on the CMM.

**Table 1.** Results of measurements (in mm) for the parts with circular holes.

|                  | Star   | Re-entrant | Gyroid | Triangular |
|------------------|--------|------------|--------|------------|
| Exterior X       | 99.812 | 99.831     | 99.794 | 99.831     |
| Exterior Y       | 99.879 | 99.740     | 99.751 | 99.858     |
| Exterior average | 99.846 | 99.786     | 99.773 | 99.845     |
| Inner circle     | 39.873 | 39.766     | 39.857 | 39.551     |

**Table 2.** Results of measurements (in mm) for the parts with square holes.

|                  | Star   | Re-entrant | Gyroid | Triangular |
|------------------|--------|------------|--------|------------|
| Exterior X       | 99.865 | 99.909     | 99.801 | 99.855     |
| Exterior Y       | 99.898 | 99.775     | 99.825 | 99.869     |
| Exterior average | 99.882 | 99.842     | 99.813 | 99.862     |
| Inner X          | 29.998 | 30.078     | 29.990 | 29.839     |
| Inner Y          | 30.093 | 30.033     | 30.110 | 29.684     |
| Inner average    | 30.045 | 30.055     | 30.050 | 29.792     |

For the parts with circular holes, measurements were taken following two different approaches. The first one (discrete) is about measuring the diameter between two opposing points on the periphery of the hole. This is repeated 18 times and the average diameter is noted. In the second one (circumferential), the probe of the CMM travels over the periphery of the hole. The resulting diameters obtained by the circumferential method demonstrated acceptable results than the other discrete approach. This is due to

**Table 3.** Results of measurements (in mm) at different heights for the parts with circular holes.

|              | Height | Star   | Re-entrant | Gyroid | Triangular |
|--------------|--------|--------|------------|--------|------------|
| Exterior X   | 2      | 99.787 | 99.776     | 99.771 | 99.746     |
|              | 5      | 99.802 | 99.850     | 99.754 | 99.820     |
|              | 8      | 99.846 | 99.866     | 99.858 | 99.927     |
| Exterior Y   | 2      | 99.853 | 99.657     | 99.703 | 99.781     |
|              | 5      | 99.857 | 99.738     | 99.690 | 99.846     |
|              | 8      | 99.926 | 99.824     | 99.860 | 99.946     |
| Inner circle | 2      | 39.920 | 39.807     | 39.833 | 39.525     |
|              | 5      | 39.876 | 39.757     | 39.845 | 39.542     |
|              | 8      | 39.824 | 39.735     | 39.893 | 39.586     |

**Table 4.** Results of measurements (in mm) at different heights for the parts with square holes.

|            | Height | Star   | Re-entrant | Gyroid | Triangular |
|------------|--------|--------|------------|--------|------------|
| Exterior X | 2      | 99.835 | 99.918     | 99.774 | 99.797     |
|            | 5      | 99.857 | 99.915     | 99.747 | 99.838     |
|            | 8      | 99.901 | 99.893     | 99.881 | 99.930     |
| Exterior Y | 2      | 99.885 | 99.717     | 99.827 | 99.822     |
|            | 5      | 99.899 | 99.761     | 99.786 | 99.849     |
|            | 8      | 99.910 | 99.848     | 99.861 | 99.935     |
| Inner X    | 2      | 29.991 | 30.054     | 29.990 | 29.873     |
|            | 5      | 30.019 | 30.091     | 30.014 | 29.828     |
|            | 8      | 29.985 | 30.090     | 29.964 | 29.814     |
| Inner Y    | 2      | 30.094 | 30.051     | 30.083 | 29.720     |
|            | 5      | 30.092 | 30.049     | 30.142 | 29.670     |
|            | 8      | 30.093 | 30.000     | 30.105 | 29.662     |

the fact that for the discrete approach, low-quality regions on the inner face of the hole encountered during the measurement have greater effects on the average diameter value than the circumferential one. The measurement results showed that the parts with star honeycomb and gyroid infill structures tend to demonstrate better accuracy when the average diameter of the holes is considered. For example, deviation from the reference diameter for the parts with star honeycomb infill is nearly 28% of the parts with triangular infill. This is due to the symmetric nature of these infill structures as opposed to the re-entrant honeycomb and triangular infills. In addition to the symmetry, increasing the number of connection points to the inner circle has a positive effect on the behavior of the parts in terms of dimensional accuracy. Even though the part with star honeycomb infill has significantly less number of connection points on the inner hole than the part with gyroid infill, the accuracy of the inner diameters of these parts is similar. Moreover, the parts with triangular infill are the least accurate among others.

For the parts with square holes, measurements were taken with an interval of 5 mm for the opposite faces of the square. When the averages of these measurements are considered, the best results were obtained with the star honeycomb pattern. However, parts with re-entrant honeycomb and gyroid infills indicate nearly the same results as the part having star honeycomb infill. In addition to this, in the y-axis, the re-entrant honeycomb infill structure showed superior dimensional accuracy compared to the parts with square holes. Deviation from the reference dimension for this infill is nearly three times less than its closest competitor. However, because of its asymmetric arrangement, its performance on the x-axis falls behind compared to the star honeycomb and gyroid infill structures. Regarding circular holes, measurements of the part having a triangular infill structure are the least satisfactory ones for the case of square holes. For example, deviation from the reference for the dimensions of the inner rectangle for the parts with triangular infill is approximately four times more than the parts with other infills.

As another observation, for all the printed parts, greater accuracy was achieved for square holes than the circular ones. Since the star honeycomb, re-entrant honeycomb and gyroid patterns are aligned with the x and y axes of the parts, having a circular inner feature in them breaks the uniformity of these infill structures and the angles of the connecting lines vary. This affects the shrinkage behavior of the structure at different angles. However, in the case of square holes, the orientations of the connecting lines do not change with the angle, resulting in structures having more homogeneous patterns.

### 3 Conclusions and Future Works

This study aimed to develop a design methodology to increase the dimensional accuracy of parts manufactured via FFF-type 3D printers. In the FFF process, extruded material is immediately cooled with the help of the fans (forced convection), and later it is further cooled down to the room temperature (natural convection). These two cooling steps result in volumetric shrinkage of the extruded beads which has a negative effect on the dimensional accuracy of the 3D printed parts. This study focused on examining the effects of different infill structures, especially the auxetics, on the shrinkage behavior of 3D printed parts. Some important outcomes of this study are as follows.

- Using auxetics as the infill pattern increases the dimensional accuracy of parts.
- When the accuracy of the outer dimensions of the parts was considered, the best results were obtained for the parts having star honeycomb infill structures. Moreover, outer dimensions of the parts with re-entrant honeycomb infill have considerable differences due to the asymmetric nature of their infill.
- For the circular inner features, the method of circumferential measurement demonstrated better accuracy than the discrete method.
- Star honeycomb and gyroid infill structures demonstrated better performance in terms of dimensional accuracy of the inner hole. This conclusion was expected due to the symmetric nature of these infill structures and higher number of connection points on the inner hole in the gyroid infill.
- Regarding the inner rectangular feature, the best results were obtained with the star honeycomb infill. However, other infill structures except the triangular one demonstrated similar results with the star honeycomb infill.

- Moreover, better dimensional accuracy was obtained for rectangular inner features rather than the circular ones. This is due to the fact that the rectangular internal features do not disturb the homogeneity of infill patterns.

As a future work, it is planned to propose a new design having a star honeycomb infill structure, but this infill would be denser than the parts manufactured in this study. Other possible studies would be examining the effects of built platform temperature on the shrinkage behavior of 3D printed parts and determining the optimum temperature to increase the dimensional accuracy of the parts.

**Acknowledgements.** This work is supported in part by Middle East Technical University under the project contract GAP-302-2018-2833.

## References

1. Dilberoglu, U.M., Simsek, S., Yaman, U.: Shrinkage compensation approach proposed for ABS material in FDM process. *Mater. Manuf. Process.* **34**, 993–998 (2019)
2. Sood, A.K., Ohdar, R.K., Mahapatra, S.S.: Improving dimensional accuracy of fused deposition modelling processed part using grey Taguchi method. *Mater. Des.* **30**(10), 4243–4252 (2009)
3. Yaman, U.: Shrinkage compensation of holes via shrinkage of interior structure in FDM process. *Int. J. Adv. Manuf. Technol.* **94**, 2187–2197 (2017). <https://doi.org/10.1007/s00170-017-1018-2>
4. Schmutzler, C., Zimmermann, A., Zaeh, M.F.: Compensating warpage of 3D printed parts using free-form deformation. *Procedia CIRP* **41**, 1017–1022 (2016)
5. Choi, Y., Kim, C., Jeong, H., Youn, J.: Influence of bed temperature on heat shrinkage shape error in FDM additive manufacturing of the ABS-engineering plastic. *World J. Eng. Technol.* **4**, 186–192 (2016)
6. Noriega, A., Blanco, D., Alvarez, B.J., Garcia, A.: Dimensional accuracy improvement of FDM square cross-section parts using artificial neural networks and an optimization algorithm. *Int. J. Adv. Manuf. Technol.* **69**(9–12), 2301–2313 (2013). <https://doi.org/10.1007/s00170-013-5196-2>
7. Huang, Q., Zhang, J., Arman, S., Thirhnakar, D.: Optimal offline compensation of shape shrinkage for three-dimensional printing processes. *IIE Trans.* **47**, 431–441 (2015)
8. Alomarah, A., Ruan, D., Masood, S., Gao, Z.: Compressive properties of a novel additively manufactured 3D auxetic structure. *Smart Mater. Struct.* **28**(8) (2019)
9. History of Sandwich Construction and Honeycombs. <https://www.econhp.de/history.html>. Accessed 14 Feb 2021
10. Hassanin, H., Abena, A., Elsayed, M.A., Essa, K.: 4D printing of NiTi auxetic structure with improved ballistic performance. *Micromachines* **11**(8), 745 (2020)
11. Maran, S., Masters, I.G., Gibbons, G.J.: Additive manufacture of 3D auxetic structures by laser powder bed fusion—design influence on manufacturing accuracy and mechanical properties. *Appl. Sci.* **10**(21), 7738 (2020)
12. Wagner, M., Chen, T., Kristina, S.: Large shape transforming 4D auxetic structures. *Mater. Des.* **4**(3), 133–142 (2017)
13. Lvov, V.A., Senatov, F.S., Korsunsky, A.M., Salimon, A.I.: Design and mechanical properties of 3D-printed auxetic honeycomb structure. *Mater. Today Commun.* **24** (2020)